Gold ion implantation induced high conductivity and enhanced electron field emission properties in ultrananocrystalline diamond films

K. J. Sankaran, H. C. Chen, B. Sundaravel, C. Y. Lee, N. H. Tai, and I. N. Lin

Citation: Applied Physics Letters **102**, 061604 (2013); doi: 10.1063/1.4792744
View online: http://dx.doi.org/10.1063/1.4792744
View Table of Contents: http://scitation.aip.org/content/aip/journal/apl/102/6?ver=pdfcov
Published by the AIP Publishing

Gold ion implantation induced high conductivity and enhanced electron field emission properties in ultrananocrystalline diamond films

K. J. Sankaran,[1] H. C. Chen,[2] B. Sundaravel,[3] C. Y. Lee,[1] N. H. Tai,[1,a)] and I. N. Lin[2,b)]
[1]*Department of Materials Science and Engineering, National Tsing-Hua University, Hsinchu 300, Taiwan*
[2]*Department of Physics, Tamkang University, Tamsui 251, Taiwan*
[3]*Materials Science Group, Indira Gandhi Centre for Atomic Research, Kalpakkam 603 102, India*

(Received 2 January 2013; accepted 6 February 2013; published online 15 February 2013)

We report high conductivity of 185 $(\Omega\,\mathrm{cm})^{-1}$ and superior electron field emission (EFE) properties, viz. low turn-on field of 4.88 V/μm with high EFE current density of 6.52 mA/cm^2 at an applied field of 8.0 V/μm in ultrananocrystalline diamond (UNCD) films due to gold ion implantation. Transmission electron microscopy examinations reveal the presence of Au nanoparticles in films, which result in the induction of nanographitic phases in grain boundaries, forming conduction channels for electron transport. Highly conducting Au ion implanted UNCD films overwhelms that of nitrogen doped ones and will create a remarkable impact to diamond-based electronics. [http://dx.doi.org/10.1063/1.4792744]

Electron field emission (EFE) from carbon and related materials has received great attention due to the immense potential of this material to be employed as a cold cathode material in flat panel displays and other electron field emitting devices.[1–3] Among field emitting materials, diamond is known as a fascinating electronic material due to its negative electron affinity (NEA) surface.[4–6] It is also known for its unique physical and chemical properties and high thermal conductivity that can promote devices with higher efficiencies.[7–9] Recently, ultrananocrystalline diamond (UNCD) films have attracted significant attention from researchers because of their unique granular structure.[10] While the grains of UNCD films have sp^3 character, the grain boundaries have a mixture of sp^2, sp^3, hydrocarbon and amorphous carbon, in which the sp^2 character is predominant.[11] The great promise that a diamond or an UNCD film bears as a material for the fabrication of cold cathode or other electron emitting devices requires the film to be conductive. The incorporation of N_2 into UNCD film's growth plasma can effectively improve the electrical conductivity and the EFE properties of the films. This is because N_2 give rise to a conversion of an amorphous phase to a graphite phase at the grain boundaries, increasing the number of percolative conduction paths in the material.[12–15] It indicates that the grain boundary conduction mechanism is responsible for the observed increase in conductivity of N_2 doped UNCD films, while nano-sized diamond grains give little contribution to the conductivity. Nevertheless, the N_2 doping temperature to create conductivity for UNCD films is very high (about 800 °C).[16,17]

Ion implantation has long been used to modify the properties of materials through controlled doping with a variety of dopants.[18–20] The C-C and hydrocarbon bonds can be broken in the ion implantation process to form sp^2 carbon. The sp^2 bonded carbon in diamond films can be thought of as electrical conduction promoters, particularly if the sp^2 bonds form interconnected networks along, which electrons are free to move. Recent reports showed that oxygen and phosphorous ion implantation on UNCD films provides n-type conductivity, which is mediated by current paths supplied to the films by the amorphous carbon (*a-C*) grain boundaries.[21,22] However, the electrical conductivity of *a-C* phases contained in the grain boundaries of UNCD films is not sufficiently high and, therefore, limits the EFE properties attainable for UNCD films.[23]

Here, we report the positive effect of Au ion implantation to enhance the conductivity and the EFE properties of UNCD films. The modifications to the microstructure of these films due to Au ion implantation were investigated in detail using transmission electron microscopy (TEM), and the role played by the implanted Au ions to enhance the EFE properties of conducting UNCD films is discussed.

The UNCD films with ultra-smooth surface characteristics at nanoscale prepared for Au ion implantation were grown on n-type silicon substrates by microwave plasma enhanced chemical vapor deposition system (IPLAS, Cyrannus), using Ar(99%)/CH_4(1%) gas at 1200 W and 120 Torr. Prior to the growth of UNCD films, the substrates were ultrasonicated for 45 min in methanol solution containing the mixture of diamond nano-powder (about 4 nm in size) and Ti powder (SIGMA-ALDRICH) (365 mesh) to facilitate the nucleation process. The growth process was carried out at low substrate temperature without any intentional heating of the substrate. The substrate temperature was estimated to be around 475 °C with a thermocouple attached to the substrate holder. The films were grown for 240 min to reach a thickness of 650 nm, which was confirmed from the cross-sectional field emission scanning electron microscopy (FESEM; JEOL 6500) image (figure not shown). Gold ion implantation was performed at room temperature with implantation energy of 500 keV, which corresponds to a projected range of 80.3 ± 8.6 nm as given by SRIM2003.[24] The ion dosages are varied from 1×10^{15} to 1×10^{17} ions/cm^2 at an ion flux of 1.035×10^{12} ions/cm^2/s. The pristine UNCD films are designated as Au0 and the films, which have undergone implantations using ion doses of

a)Electronic mail: nhtai@mx.nthu.edu.tw.
b)Electronic mail: inanlin@mail.tku.edu.tw.

1×10^{15}, 1×10^{16}, 1×10^{17} ions/cm^2 are called Au15, Au16, and Au17 samples, respectively.

The secondary ion mass spectroscopy (SIMS, Cameca-I4f) depth profile shown in Fig. 1 suggests that Au is implanted into UNCD to a depth of about 320 nm with peak concentration located at around 160 nm beneath the surface. The peak around 160 nm is almost twice of the projected range of 500 keV Au ions, which can be attributed to radiation enhanced diffusion of implanted ions.[25,26] This profile confirms that Au ions have been implanted in the UNCD films. The Hall measurements were carried out in a van der Pauw configuration (ECOPIA HMS-3000) to examine the conducting behavior of the Au ion implanted UNCD films. The electrical conductivity of the Au ion implanted UNCD films are plotted in Fig. 2(a) as solid squares. The Au0 films are too resistive to be measured using the van der Pauw configuration. Interestingly, the electrical conductivity of Au ion implanted UNCD films increases monotonously with increasing ion dosage, from 0.03 $(\Omega\ \text{cm})^{-1}$ (carrier concentration of $n = 2.07 \times 10^{15}\ \text{cm}^{-2}$ and mobility of $\mu = 1.2 \times 10^2\ \text{cm}^2/\text{V s}$) for Au15 films to about 185 $(\Omega\ \text{cm})^{-1}$ ($n = 5.50 \times 10^{20}\ \text{cm}^{-2}$ and $\mu = 8.5 \times 10^2\ \text{cm}^2/\text{V s}$) for Au17 films. The obtained electrical conductivity and carrier concentration values of Au17 films are comparable with those of high temperature (700 °C) grown nitrogen doped UNCD films[14,15] and are superior to that of the phosphorous and oxygen ion implanted UNCD films[21,22] (see, Table I).

The EFE characteristics of the samples were measured in an electrical field using a parallel plate configuration, where a molybdenum rod with a diameter of 2 mm was used as anode. The current density versus electrical field (J_e-E) characteristics was acquired using a Keithley 237 electrometer. The EFE characteristics of materials were explained using the Fowler Nordheim (FN) theory,[27] as shown in Fig. 2(b), where the EFE properties of the Au0 films were included as curve I to facilitate the comparison. The turn-on field (E_0) is designated as the interception of the straight lines extrapolated from the low field and the high field segments of the FN plots [inset of Fig. 2(b)], viz. $\log(J_e/E^2)$-$1/E$. The Au0 films exhibit the largest E_0 of 19.33 V/μm with the lowest J_e of 1.03 mA/cm^2 at an applied field of 33.5 V/μm [curve I, Fig. 2(b)]. The E_0 value decreases consistently with

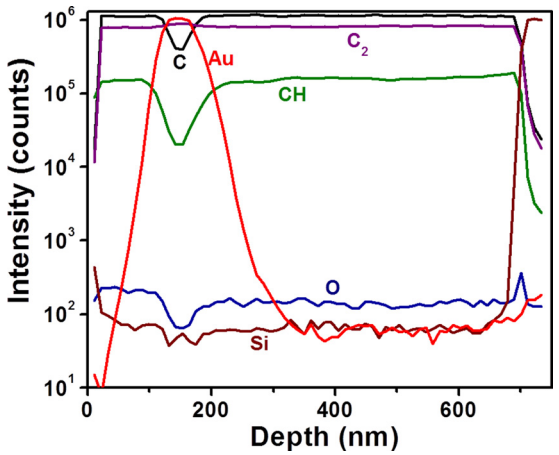

FIG. 1. SIMS depth profiles of C, C_2, CH, Au, Si, and O species in Au17 films.

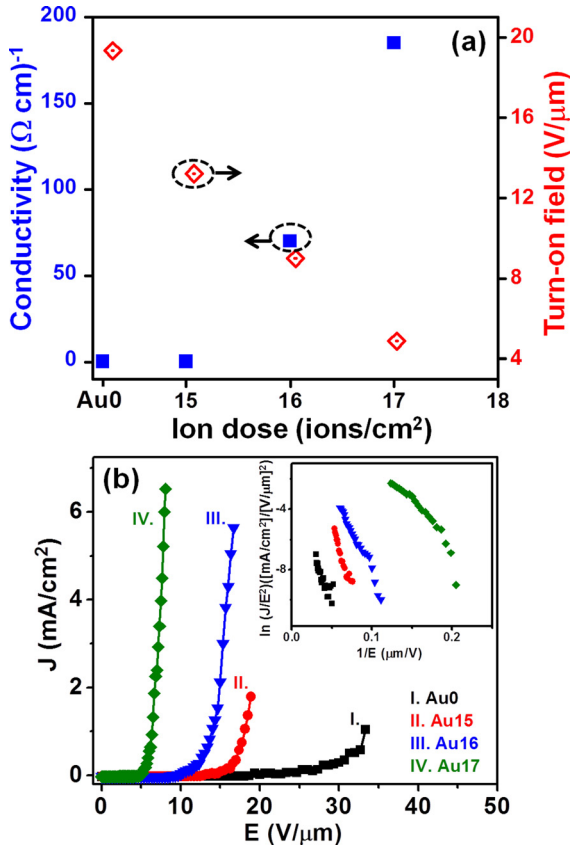

FIG. 2. (a) Variation in the electrical conductivity (solid squares) and turn-on field (open circles) and (b) the electron field emission properties of UNCD films with varying Au ion dose. (The pristine UNCD film is designated as Au0).

the dosage of Au ion implantation [open circles, Fig. 2(a)]. The Au17 films show the best EFE characteristics, i.e., the lowest E_0 of 4.88 V/μm and the highest J_e of 6.52 mA/cm^2 at an applied field of 8.0 V/μm [curve IV, Fig. 2(b)]. The EFE properties of Au17 films are better than those of conducting UNCD films ever reported (see, Table I).

The implantation of Au ions (1×10^{17} ions/cm^2) induces dramatic changes in the surface microstructure of the UNCD films as a featureless surface morphology for Au17 films from a equi-axed ultra-small granular structure of Au0 films, as shown in Figs. 3(a) and 3(b), respectively. The energy dispersive X-ray spectroscopy (EDX) spectrum corresponding to the FESEM image of Au17 films [inset I, Fig. 3(a)] clearly shows the Au peak indicating Au presence in the films, whereas the spectrum corresponding to the Au0 films shows the presence of C and Si only [inset I, Fig. 3(b)]. The bonding character of different types of carbon in the UNCD films

TABLE I. Comparison on the electrical conductivity measured and turn-on field of electron field emission for the conducting UNCD films.

Materials	Electrical conductivity $(\Omega\ \text{cm})^{-1}$	Turn-on field (V/μm)	References
N_2 doped UNCD	200	6.13	14 and 15
O_2 ion implanted UNCD	33.3	…	21
P ion implanted UNCD	0.09	…	22
Au ion implanted UNCD	185	4.88	This study

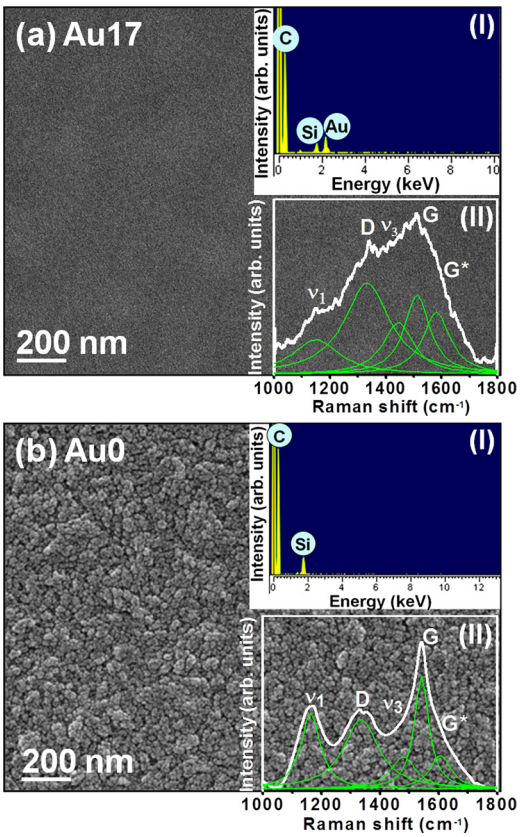

FIG. 3. FESEM images of UNCD surfaces with inset I show the EDX spectrum for the elemental composition of the corresponding FESEM image and the inset II shows the Raman spectrum of (a) Au17 and (b) Au0 films.

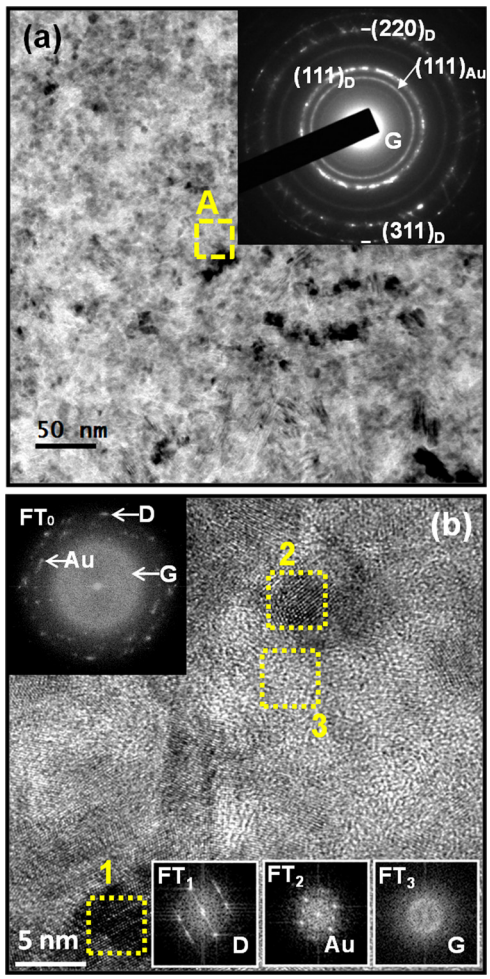

FIG. 4. (a) TEM micrograph with corresponding SAED pattern shown as inset and (b) high resolution TEM structure image corresponding to region A in (a). The FT image corresponding to whole structure image is shown as FT_0 and the FT images of the selected regions marked as 1–3 are shown as insets the FT_1–FT_3 images, respectively.

is characterized by Raman spectroscopy [Lab Raman HR800, Jobin Yvon; $\lambda = 632$ nm, inset II, Figs. 3(a) and 3(b)]. The inset II in Fig. 3(b) shows the visible-Raman spectrum of Au0 films that is deconvoluted using the multi-peak Lorentzian fitting method. The spectrum contains the ν_1-band (1163 cm^{-1}) and the ν_3-band (1478 cm^{-1}) resonance peaks, which correspond to *trans*-polyacetylene at the grain boundaries,[28,29] and the D-band (1333 cm^{-1}) and the G-band (1538 cm^{-1}) resonance peaks, which correspond to disordered carbon.[30,31] The sharp peak at 1332 cm^{-1}, which is commonly observed for microcrystalline diamond films, is not observed for the Au0 films because visible-Raman is more sensitive to sp^2 bonded carbons, as compared to the sp^3 bonds.[10] The Raman spectrum is markedly altered by the Au ion implantation [inset II, Fig. 3(a)]. The higher intensities of D (1344 cm^{-1}) and G peaks (1542 cm^{-1}) indicate amorphization and graphitization types, respectively, of transitions in the UNCD films due to Au ion implantation.[18] A shoulder peak (G*) near 1600 cm^{-1} possibly arises from the nanocrystalline graphitic content in the films.[31] The G-band resonance peak shifts to the wavenumber higher than that of the conventional graphite peaks (1538 cm^{-1}), confirming the formation of nanographite.

To elucidate how highly conducting UNCD materials are formed due to Au ion implantation, the microstructure of the Au17 films were investigated using TEM (JEOL-2100F, 200 eV). Fig. 4(a) shows the typical TEM image of Au17 films. Selective area electron diffraction (SAED) pattern shown in the inset of Fig. 4(a) illustrates that, besides the diffraction rings corresponding to the $(111)_D$, $(220)_D$, and $(311)_D$ lattice planes of diamond, there is a presence of an extra diffraction ring corresponding to Au material. Such an observation indicates that these regions contain abundant nanosized Au particles uniformly distributed among the diamond grains. This observation is in accord with the FESEM-EDX elemental analysis results [inset I, Fig. 3(a)]. There also exist some graphitic (or *a-C*) phases in these films that is verified by the prominent diffused ring in the center of this SAED.

More detailed investigations were carried out on the Au17 films by high resolution TEM studies for the identification of different phase constituents. Fig. 4(b) shows the structure image for Au17 films corresponding to region A in Fig. 4(a). Fourier transformed (FT) image of the whole structure image (FT_0) shows a spotted diffraction pattern arranged in ring, suggesting of nano-sized nature of the diamond (D) and the gold (Au) phases. The diffused diffraction ring located at the center of FT image corresponds to graphitic (G) phase. The existence of diamond (D) and gold (Au) phases are highlighted by regions 1 and 2, respectively, which are identified by the FT images FT_1 and FT_2, respectively. The presence of graphitic phases in the grain boundaries, highlighted by the region 3, is confirmed by the FT

image FT_3. On the basis of TEM investigations for the Au17 film, it is noticed that Au ion implantation induces the presence of nanographitic phases, in conjunction with the formation of Au nanoparticles.

Previous reports revealed that the grain boundary phases (*a-C* and graphite) coexist among the diamond grains of the UNCD films are the authentic factors for the enhancement in electrical conductivity and EFE properties of UNCD films.[15,23,32] The same conduction mechanism may be applied to account for the improved conductivity due to Au ion implantation. In this work, the Au ion implantation beneficially consequences in the formation of Au nanoparticles on the UNCD films that induces nanographitic phases in the films. Such observations are in concordance with our conduction mechanism that the electrons are transported easily through the graphitic phases as well as through the conduction channels of the diamond grains to the emitting surface and are then emitted to vacuum without any difficulty as the diamond surfaces are NEA in nature.[5,6] Consequently, the formations of Au nanoparticles and nanographitic phases exist among the diamond grains of UNCD films due to Au ion implantation are the actual factors for the enhanced EFE properties of the Au17 films.

In summary, a possible way of fabricating high field emitting conducting UNCD films due to Au ion implantation is demonstrated. The Au17 films are highly conducting as compared to Au0 films. The Au0 films show comparatively inferior EFE properties that are ascribed to the *a-C* phases formed in the boundaries of the diamond grains, which hinders the transportation of electrons. In the case of the Au17 films, the formations of Au nanoparticles and the introduction of nanographitic phases among the diamond grains advance the conducting nature of the films, which are possibly the prime reasons for the enhanced EFE properties of the Au17 films. The highly conducting Au ion implanted UNCD films with enhanced EFE characteristics may open up a pathway for the invention of high-definition flat panel displays or plasma devices.

The authors like to thank the financial support of National Science Council, Taiwan through the project Nos. NSC 99-2119-M-032-003-MY2 and NSC 101-2221-E-007-064-MY3.

[1]W. Zhu, G. P. Kochanski, and S. Jin, Science **282**, 1471 (1998).
[2]K. Okano, K. Hoshina, M. Iida, S. Koizumi, and T. Inuzuka, Appl. Phys. Lett. **64**, 2742 (1994).
[3]W. L. Wang, J. D. Fabbri, T. M. Willey, J. R. I. Lee, J. E. Dahl, R. M. K. Carlson, P. R. Schreiner, A. A. Fokin, B. A. Tkachenko, N. A. Fokina, W. Meevasana, N. Mannella, K. Tanaka, X. J. Zhou, T. van Buuren, M. A. Kelly, Z. Hussain, N. A. Melosh, and Z.-X. Shen, Science **316**, 1460 (2007).
[4]M. W. Geis, N. N. Efremow, K. E. Krohn, J. C. Twichell, T. M. Lyszczarz, R. Kalish, J. A. Greer, and M. D. Tabat, Nature **393**, 431 (1998).
[5]H. Yamaguchi, T. Masuzawa, S. Nozue, Y. Kudo, I. Saito, J. Koe, M. Kudo, T. Yamada, Y. Takakuwa, and K. Okano, Phys. Rev. B **80**, 165321 (2009).
[6]M. W. Geis, S. Deneault, K. E. Krohn, M. Marchant, T. M. Lyszczarz, and D. L. Cooke, Appl. Phys. Lett. **87**, 192115 (2005).
[7]K. Okano, S. Koizumi, S. R. P. Silva, and G. A. J. Amaratunga, Nature **381**, 140 (1996).
[8]A. Krueger, Adv. Mater. **20**, 2445 (2008).
[9]H. Watanabe, C. E. Nebel, and S. Shikata, Science **324**, 1425 (2009).
[10]T. D. Corrigan, D. M. Gruen, A. R. Krauss, P. Zapol, R. P. H. Chang, Diamond Relat. Mater. **11**, 43 (2002).
[11]J. Birrell, J. A. Carlisle, O. Auciello, D. M. Gruen, and J. M. Gibson, Appl. Phys. Lett. **81**, 2235 (2002).
[12]D. Zhou, A. R. Krauss, L. C. Qin, T. G. McCauley, D. M. Gruen, T. D. Corrigan, R. P. H. Chan, and H. Gnaser, J. Appl. Phys. **82**, 4546 (1997).
[13]J. Birrell, J. E. Gerbi, O. Auciello, J. M. Gibson, D. M. Gruen, and J. A. Carlisle, J. Appl. Phys. **93**, 5606 (2003).
[14]R. Arenal, P. Bruno, D. J. Miller, M. Bleuel, J. Lal, and D. M. Gruen, Phys. Rev. B **75**, 195431 (2007).
[15]K. J. Sankaran, J. Kurian, H. C. Chen, C. L. Dong, C. Y. Lee, N. H. Tai, and I. N. Lin, J. Phys. D: Appl. Phys. **45**, 365303 (2012).
[16]S. Bhattacharyya, O. Auciello, J. Birrell, J. A. Carlisle, L. A. Curtiss, A. N. Goyette, D. M. Gruen, A. R. Krauss, J. Schlueter, A. Sumant, and P. Zapol, Appl. Phys. Lett. **79**, 1441 (2001).
[17]Y. C. Lin, K. J. Sankaran, Y. C. Chen, C. Y. Lee, H. C. Chen, I. N. Lin, and N. H. Tai, Diamond Relat. Mater. **20**, 191 (2011).
[18]R. Kalish, Carbon **37**, 781 (1999).
[19]S. Talapatra, J. Y. Cheng, N. Chakrapani, S. Trasobares, A. Cao, R. Vajtai, M. B. Huang, and P. M. Ajayan, Nanotechnology **17**, 305 (2006).
[20]S. Prawer and R. Kalish, Phys. Rev. B **51**, 15711 (1995).
[21]X. J. Hu, J. S. Ye, H. J. Liu, Y. G. Shen, X. H. Chen, and H. Hu, J. Appl. Phys. **109**, 053524 (2011).
[22]X. J. Hu, J. S. Ye, H. Hu, X. H. Chen, and Y. G. Shen, Appl. Phys. Lett. **99**, 131902 (2011).
[23]K. J. Sankaran, K. Panda, B. Sundaravel, H. C. Chen, I. N. Lin, C. Y. Lee, and N. H. Tai, ACS Appl. Mater. Interfaces **4**, 4169 (2012).
[24]J. F. Ziegler, J. P. Biersack, and U. Littmark, *The Stopping and Ranges of Ions in Solids* (Pergamon, NewYork, 1985).
[25]K. Y. Gao and B. X. Liu, J. Appl. Phys. **82**, 2209 (1997).
[26]N. D. Skelland and P. D. Townsend, J. Phys. D: Appl. Phys. **27**, 1672 (1994).
[27]R. H. Fowler and L. Nordheim, Proc. R. Soc. London, Ser. A **119**, 173 (1928).
[28]Z. Sun, J. R. Shi, B. K. Tay, and S. P. Lau, Diamond Relat. Mater. **9**, 1979 (2000).
[29]A. C. Ferrari and J. Robertson, Phys. Rev. B **63**, 121405 (2001).
[30]J. Michler, Y. Von Kaenel, J. Stiegler, and E. Blank, J. Appl. Phys. **83**(1), 187 (1998).
[31]A. C. Ferrari and J. Robertson, Phys. Rev. B **61**, 14095 (2000).
[32]K. J. Sankaran, H. C. Chen, C. Y. Lee, N. H. Tai, and I. N. Lin, Appl. Phys. Lett. **101**, 241604 (2012).